Supramolecular Chemistry
Publication details, including instructions for authors and subscription information:
http://www.informaworld.com/smpp/title~content=t713649759

Supramolecular β-Sheet and Nanofibril Formation by Self-assembling Tripeptides Containing an N-terminally Located γ-Aminobutyric acid Residue

Sudipta Ray[a]; Michael G. B. Drew[b]; Apurba Kumar Das[a]; Arindam Banerjee[a]
[a] Department of Biological Chemistry, Indian Association for the Cultivation of Science, Jadavpur, Kolkata, India [b] School of Chemistry, The University of Reading, Reading, UK

To cite this Article Ray, Sudipta , Drew, Michael G. B. , Das, Apurba Kumar and Banerjee, Arindam(2006) 'Supramolecular β-Sheet and Nanofibril Formation by Self-assembling Tripeptides Containing an N-terminally Located γ-Aminobutyric acid Residue', Supramolecular Chemistry, 18: 5, 455 — 464
To link to this Article: DOI: 10.1080/10610270600677033
URL: http://dx.doi.org/10.1080/10610270600677033

Supramolecular Chemistry, July–August 2006 Vol. 18 (5), pp. 455–464

Taylor & Francis
Taylor & Francis Group

Supramolecular β-Sheet and Nanofibril Formation by Self-assembling Tripeptides Containing an N-terminally Located γ-Aminobutyric acid Residue

SUDIPTA RAY[a], MICHAEL G. B. DREW[b], APURBA KUMAR DAS[a] and ARINDAM BANERJEE[a,*]

[a]*Department of Biological Chemistry, Indian Association for the Cultivation of Science, Jadavpur, Kolkata 700032, India;* [b]*School of Chemistry, The University of Reading, Whiteknights, Reading, RG6 6AD, UK*

(Received 14 December 2005; accepted 27 February 2006)

Three terminally protected tripeptides Boc–γ-Abu–Val–Leu–OMe 1, Boc–γ-Abu–Leu–Phe–OMe 2 and Boc–γ-Abu–Val–Tyr–OMe 3 (γ-Abu = γ-aminobutyric acid) each containing an N-terminally positioned γ-aminobutyric acid residue have been synthesized, purified and studied. FT-IR studies of all these peptides revealed that these peptides form intermolecularly hydrogen bonded supramolecular β-sheet structures. Peptides 1, 2 and 3 adopt extended backbone β-strand molecular structures in crystals. Crystal packing of all these peptides demonstrates that these β-strand structures self-assemble to form intermolecularly H-bonded parallel β-sheet structures. Peptide 3 uses a side chain tyrosyl –OH group as an additional hydrogen bonding functionality in addition to the backbone CONH groups to pack in crystals. Transmission electron microscopic studies of all peptides indicate that they self-assemble to form nanofibrillar structures of an average diameter of 65 nm. These peptide fibrils exhibit amyloid-like behavior as they bind to a physiological dye Congo red and show a characteristic green-gold birefringence under polarizing microscope.

Keywords: Self-assembly; Nanofibril; Peptide; γ-Abu

INTRODUCTION

Self-assembling systems are ubiquitous in biology. Being inspired from biology, design and construction of suitable molecular building blocks, which self-assemble to form supramolecular helices [1–3], β-sheets etc. [4–7] is a very active area of current research. The β-sheet is a biologically important structure present in many proteins. There are numerous examples of self-assembling synthetic peptides [8–17] and peptidomimetics [18,19] which form β-sheet nanofibrillar structures. Some of these self-assembling, nanofibril forming oligopeptides are also important as they can be used as responsive soft materials (hydrogels) [9,10]. A recent study from Schneider's group shows the formation of β-sheet and non-twisting nanofibrils from self-assembling *de novo* designed synthetic peptides [11]. Woolfson and his coworkers have successfully engineered the morphology of self-assembling polypeptide-based nanofibers [20]. Nonlinear peptides can be used to govern the assembly of peptide based nanostructured materials using the bottom-up approach in which peptide self-assembly and fibrillogenesis can be programmed [21]. Ionic self-complementary oligopeptides self-assemble to form β-sheet structures and nanofibers and these nanofibers under suitable conditions encapsulate a large volume of water molecules to form hydrogels comprising of $>99.5\%$ water [12]. These nanofiber scaffolds can be fragmented by sonication and reassembled to form the original-like nanofiber scaffold indicating its high potentiality for future application in tissue repair and regenerative medicine [13]. Stupp and his coworkers have nicely demonstrated the formation of nanofibers using self-assembling peptide based amphiphiles [22,23] and these peptide nanofibers can be effectively used as substrates for nucleation and growth of a semiconductor cadmium sulfide (CdS) nanocrystals [24]. Magnetic resonance active peptide amphiphiles self-assemble into nanofibers and these peptide-based nanobiomaterials can be potentially used as diagnostics in medical science [25]. Many

*Corresponding author. Fax: + 91-33-24732805 . E-mail: bcab@mahendra.iacs.res.in

ISSN 1061-0278 print/ISSN 1029-0478 online © 2006 Taylor & Francis
DOI: 10.1080/10610270600677033

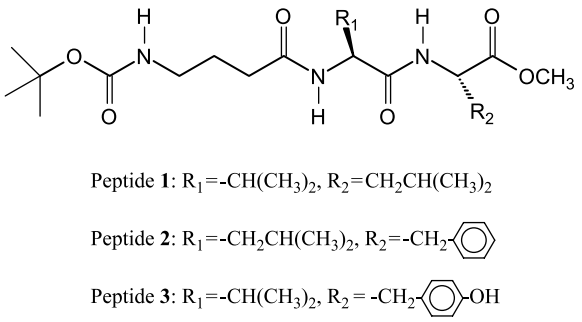

FIGURE 1 Schematic representation of peptides **1**, **2** and **3**.

fatal neurodegenerative diseases (*viz*. Alzheimer's disease, Parkinson's disease etc.) appear to be caused by the deposition of self-aggregated peptides/proteins and subsequent formation of highly ordered nanofibrillar structure, which is popularly known as amyloid fibrils. Gazit and his coworkers have made a seminal contribution in the study of self-assembling peptide based nanofibrils which show the properties of amyloid fibrils [14–16,26,27]. His group has successfully demonstrated that even small peptides like pentapeptide or tetrapeptide fragments of human calcitonin can be self-assembled to form amyloid fibrils [17]. He has also established that there is a possible role of π−π stacking in the molecular self-assembly of amyloid fibrils [28]. We are also engaged in studying synthetic self-assembling β-sheet forming short peptides, which form amyloid-like fibrils [4–7]. In this paper, we describe the molecular self-assembly of three synthetic terminally protected tripeptides **1**, **2** and **3** (Fig. 1) containing N-terminally located γ-aminobutyric acid residues. These peptides self-assemble to form β-sheet structures in crystal and also form nanofibrils that were visualized by TEM. All these peptide nanofibrils show characteristic amyloid-like behaviour.

γ-Aminobutyric acid is a non-protein, naturally occurring amino acid found in the mammalian brain [29] and acts as a neurotransmitter [30]. Each peptide in this present study contains this N-terminally located γ-aminobutyric acid (γ-Abu) residue together with an adjacently positioned valine residue for peptides **1** and **3** and leucine residue for peptide **2**. γ-Abu is a flexible γ-amino acid, which prefers to form an extended backbone conformation, when there is no contiguously positioned conformationally restricted amino acid residue like Aib (α-aminoisobutyric acid) present in the sequence [31]. The third residue for peptides **1**, **2** and **3** is leucine (Leu), phenylalanine (Phe) and tyrosine (Tyr) respectively. The bulky side chain of Leu, Phe or Tyr can help to aggregate in a self-assembling system.

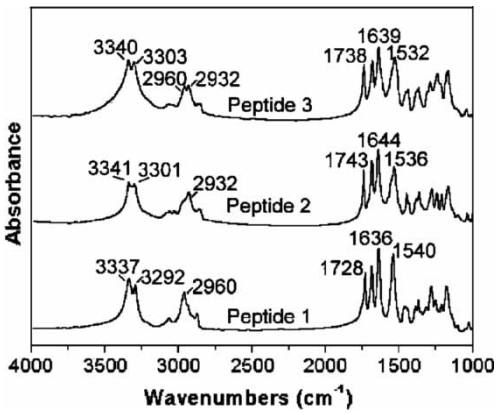

FIGURE 2 Solid state FT-IR spectra of peptides **1**, **2** and **3**.

RESULTS AND DISCUSSION

FT-IR Study

From the FT-IR study we obtained preliminary information about the conformational features of all peptides in solid state. In the solid state (using KBr matrix) intense bands lying between 3292–3341 cm^{-1} have been observed for all three peptides, which indicates the presence of strongly hydrogen bonded NH groups (Fig. 2). No band has been observed around 3400 cm^{-1} for any of the three peptides in the solid state. An absence of this band suggests that all NHs for all three peptides in solid state are involved in intermolecular hydrogen bonding. The CO stretching band at around 1636–1644 cm^{-1} (amide I) and the NH bending and the C–N stretching peak near 1532–1540 cm^{-1} suggest the presence of intermolecularly hydrogen bonded supramolecular β-sheet conformation for all peptides in the solid state [32]. So, it can be concluded from the above FT-IR data, that all peptides share this common structural feature.

X-ray Structural Analysis

Single crystals suitable for an X-ray diffraction study of peptides **1, 2** and **3** were grown from methanol–water solution by slow evaporation. Important crystallographic information for all three peptides is listed in Table I. All three peptides adopt extended backbone molecular conformations (Fig. 3). According to Table II only the torsion angles of the second amino acid in the three peptides fall within the β-sheet region of the Ramachandran Map [33]. The torsions about the methylene groups of the γ-Abu (namely θ_1 and θ_2) in peptides **1**, **2** and **3** are in the extended region. This facilitates the easy accommodation of CH_2 groups into the β-sheet conformations for all three peptides. For peptide **1** individual molecules self-assemble via intermolecular hydrogen bonds N(11) and O(10) (x, y + 1, z), N(8) and O(7) (x, y − 1, z) and N(3) and O(2) (x, y + 1, z)

TABLE I Crystallographic data for peptides Boc–γ-Abu(1)–Val(2)–Leu(3)–OMe **1**, Boc–γ-Abu(1)–Leu(2)–Phe(3)–OMe **2** and Boc–γ-Abu(1)–Val(2)–Tyr(3)–OMe **3**.

	Peptide **1**	Peptide **2**	Peptide **3**
Formula	$C_{21}H_{39}N_3O_6$	$C_{25}H_{39}N_3O_6$	$C_{24}H_{37}N_3O_7$
Formula Weight	429.55	477.59	479.57
Crystallizing solvent	Methanol–water	Methanol–water	Methanol–water
Crystal system	Orthorhombic	Monoclinic	Monoclinic
Space group	$P2_12_12_1$	$P2_1$	$P2_1$
a (Å)	14.337(17)	5.028(7)	15.886(17)
b (Å)	4.957(7)	19.210(22)	4.989(7)
c (Å)	36.51(4)	14.391(16)	17.898(19)
β (Å)	(90)	93.35(1)	107.29(1)
ν (Å^3)	2594(6)	1387(3)	1354(3)
Z	4	2	2
D_{calcd} (g cm $^{-3}$)	1.099	1.143	1.176
No of independent reflections	4276	4429	4820
Reflections with $I > 2s(I)$	1290	1731	3305
No of Parameters	279	313	315
$R1$ ($I > (2s(I))$	0.0607	0.0653	0.1014
$wR2$ ($I > 2s(I)$)	0.10441	0.0826	0. 1734
Max and Min Residual electron density, eÅ^{-3}	0.153, −0.193	0.148, −0.125	0.249, −0.234

of 3.027, 2.944, 2.862 Å respectively (Table III) and other non-covalent interactions to form an infinite parallel β-sheet assemblage in the crystal along the screw axis parallel to the crystallographic *b* direction (Fig. 4). These individual β-sheet columns are themselves regularly stacked *via* van der Waals' interactions to form a complex quaternary supramolecular sheet structure along the crystallographic *c* direction.

The crystal structure of peptide **2** shows that it adopts an infinite parallel β-sheet structure through intermolecular hydrogen bonding. There are three intermolecular hydrogen bonds between N(4) and O(3) (x − 1, y, z), N(9) and O(81) (x + 1, y, z) and N(12) and O(11) (x − 1, y, z) with donor–acceptor distances of 2.855 Å, 3.048 Å and 2.953 Å respectively (Table III). These intermolecular hydrogen bonds help in the formation of a parallel β-pleated sheet along the crystallographic *a* direction. Each β-sheet layer is then regularly packed along crystallographic *b* axis by using van der Waals' interactions (Fig. 5) to form a complex quaternary β-sheet structure.

The X-ray crystal structure of peptide **3** shows some different structural features from that of peptides **1** and **2**. This is due to the presence of the phenolic –OH group in the Tyr residue. Each molecule of peptide **3** is connected with neighboring molecules through three intermolecular hydrogen bonds between N(5) and O(6) (x, y + 1, z), N(11) and O(13) (x, y − 1, z) and N(17) and O(18) (x, y − 1, z) with a donor acceptor distance of 2.972 Å, 3.014 Å and 2.861 Å respectively, to construct an infinite parallel β-sheet structure (Table III) along crystallographic *b* axis (Fig. 6). Interestingly, one such parallel β-sheet is linked with another neighboring β-sheet by an intermolecular hydrogen bond between O(48) and O(48) (2 − x, y − 0.5, 2 − z) with a donor–acceptor distance of 2.864 Å, to form a complex quaternary β-sheet structure.

Morphological Study

The morphological studies of all three reported peptides were done by transmission electron microscope (TEM). The TEM picture of peptide **1** shows linear nanofibrillar structure with an average diameter of 65 nm (Fig. 7a). Similarly, the TEM image of peptide **2** exhibits nanofibrillar structure (Fig. 7b). Peptide **3** forms linear and also helically twisted

TABLE II Selected torsion angles* (deg) in peptides Boc–γ-Abu(1)–Val(2)–Leu(3)–OMe **1**, Boc–γ-Abu(1)–Leu(2)–Phe(3)–OMe **2** and Boc–γ-Abu(1)–Val(2)–Tyr(3)–OMe **3**.

Peptide	Residue	ϕ	Ψ	ω	θ_1	θ_2
Peptide **1**	γ-Abu	108.5(8)	−101.5(6)	170.4(6)	−175.5(5)	−176.0(7)
	Val	−116.4(6)	107.7(5)	169.7(5)		
	Leu	48.3(7)	45.3(6)	−172.2(5)		
Peptide **2**	γ-Abu	102.7(5)	−113.3(5)	−177.6(5)	−174.0(4)	−175.5(4)
	Leu	−110.4(5)	111.9(5)	177.2(5)		
	Phe	−96.6(6)	154.7(5)	−179.5(5)		
Peptide **3**	γ-Abu	79.4(7)	96.1(6)	179.8(5)	179.7(5)	172.0(5)
	Val	−121.1(5)	115.2(5)	176.5(5)		
	Tyr	−110.6(5)	68.4(6)	−168.0(4)		

*The torsion angles for rotation about the bonds of peptide backbone: ϕ, Ψ, ω. Torsions in the main chain in the N-terminal γ-Abu residue about C^α–C^β and C^β–C^γ: θ_2 and θ_1 respectively.

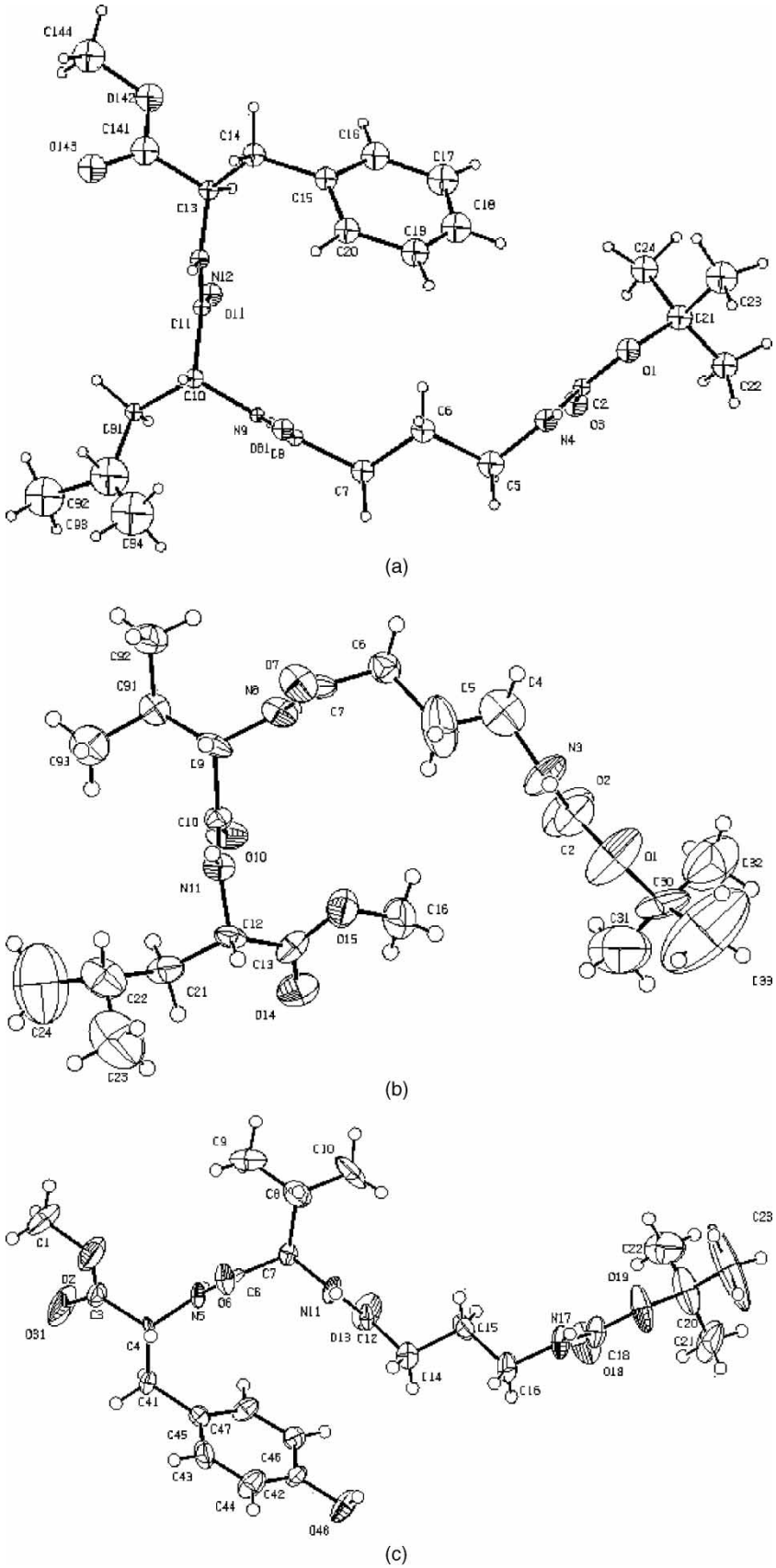

FIGURE 3 The ORTEP diagrams of (a) peptide **1,** (b) peptide **2** and (c) peptide **3** with atomic numbering schemes. Ellipsoids are at 20% probability for peptides **1** and **2** and 30% probability for peptide **3**.

TABLE III Intermolecular hydrogen-bonding parameters for peptides **1**, **2** and **3**.

D–H···A	H···A (Å)	D···A (Å)	D–H···A (Å)	Symmetry element
Peptide 1				
N3–H3···O2	2.04	2.862(8)	160	a
N8–H8···O7	2.09	2.944(7)	173	b
N11–H11···O10	2.17	3.027(7)	172	a
Peptide 2				
N4–H4···O3	2.04	2.855(8)	156	c
N9–H9···O81	2.19	3.048(9)	173	d
N12–H12···O11	2.10	2.953(9)	171	c
Peptide 3				
N5–H5···O6	2.14	2.972(9)	163	a
N11–H11···O13	2.16	3.014(10)	171.	b
N17–H17···O18	2.02	2.861(11)	165	b
O48–H48···O48	2.05	2.864(11)	171	e

[a] Symmetry element x, 1 + y, z. [b] Symmetry element x, −1 + y, z. [c] Symmetry element −1 + x, y, z. [d] Symmetry element 1 + x, y, z. [e] Symmetry element 2 − x, 1/2 + y, 2 − z.

nanofibril (Fig. 7c). These nanofibils obtained from self-assembling peptides **1**, **2** and **3** bind to a physiological dye Congo red and exhibit a characteristic green-gold birefringence when observed under a cross-polarizer (Fig. 8), a characteristic feature of amyloid fibrils [34].

The FT-IR studies as well as crystal structure analyses reveal that these reported peptides self-assemble to form intermolecularly hydrogen-bonded β-sheet structures. All these peptides on further self-assembly form nanofibrillar structures. These nanofibrillar structures are capable to bind with a physiological dye Congo red and exhibit specific birefringence under cross polarizer showing their similarities with amyloid fibrils.

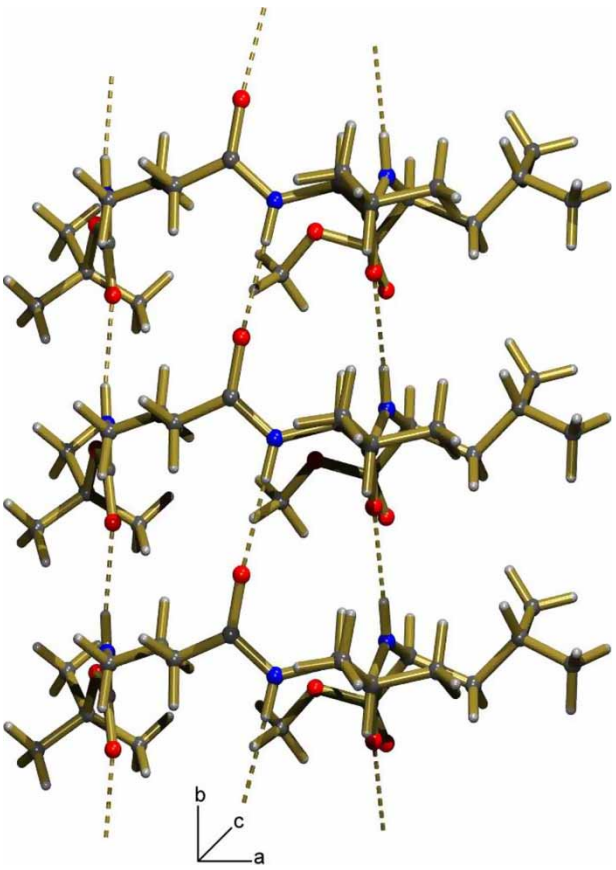

FIGURE 4 Crystal packing of peptide **1** showing the formation of a supramolecular parallel β-sheet structure along the crystallographic *b*-axis. Nitrogen atoms are blue and oxygen atoms are red. Hydrogen bonds are shown as dotted lines.

CONCLUSIONS

All terminally protected synthetic tripeptides share a common structural motif, an extended backbone β-strand molecular conformation without any intramolecular hydrogen bonded bend structure. In crystals, each molecular strand self-assembles to form a parallel β-sheet structure using various non-covalent interactions including intermolecular hydrogen bonding. The relatively fast evaporation of peptide solution leads to form nanoscale fibrils that were visualized by TEM. Peptides **1** and **2** form non-helical linear nanofibrils, while the peptide **3** forms linear and also helically twisted nanofibrils. Various factors including the amino acid sequence, concentration of the peptide, molecular size of the peptide, ionic strength *etc.* may govern the

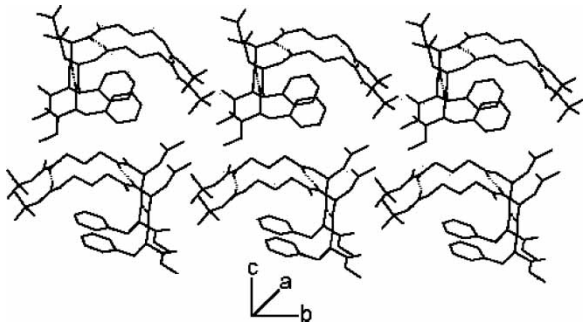

FIGURE 5 The higher order packing of peptide **2** illustrating the intermolecular hydrogen bonded supramolecular parallel β-sheet structure along the crystallographic *b* direction. Hydrogen bonds are shown as dotted lines. Non hydrogen bonded hydrogen atoms are omitted for clarity.

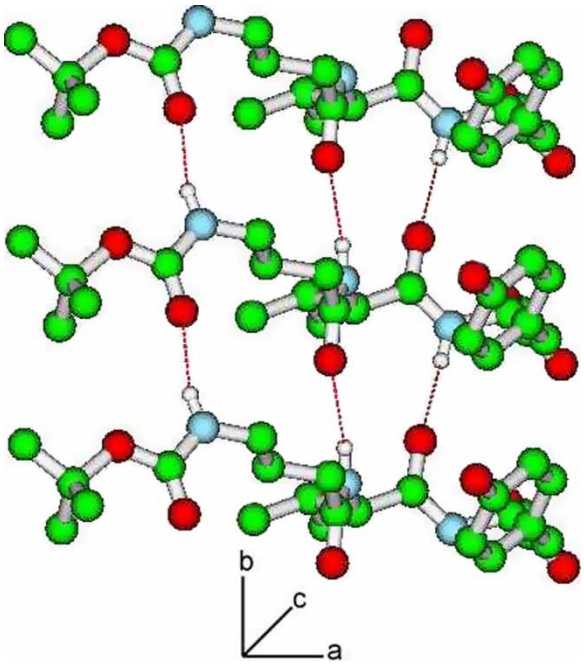

FIGURE 6 The packing of peptide **3** illustrating the intermolecular hydrogen bonded supramolecular parallel β-sheet structure along crystallographic *b* direction. Nitrogen atoms are blue, oxygen atoms are red and carbon atoms are green. Non-hydrogen bonded hydrogen atoms are omitted for clarity.

morphology of nanofibrils obtained from self-assembling oligopeptides. The morphology of nanofibrils can be tuned using self-assembling branched polypeptides [21,35]. Here, the amino acid sequence in short peptides may play a role in nanofibrillation and controlling its morphology. In the present case, the exact cause of nanofibrillation and exhibiting different morphologies (helical and linear) for different peptides are yet to explored. Moreover, these nanofibrils exhibit amyloid-like behavior as they bind to a physiological dye Congo red and show a typical birefringence when viewed through a cross-polarizer. This indicates that these self-assembling short peptide based nanofibrils may have some biological significance.

EXPERIMENTAL

Peptide Synthesis

Peptides **1, 2** and **3** were synthesized by conventional solution phase methods by using racemization free fragment condensation strategy [36]. The Boc group was used for N-terminal protection and the C-terminus was protected as a methyl ester. Deprotections were performed using saponification method. Couplings were mediated by dicyclohexylcarbodiimide/1-hydroxybenzotriazole (DCC–HOBt). All the final compounds were fully characterized by IR spectroscopy, 300 MHz ^{1}H-NMR spectroscopy and mass spectrometry.

(a) Synthesis of Boc–γ-Abu–OH **4**: See ref [31].

(b) Boc–γ-Abu(1)–Val(2)–OMe **5**: 4.06 g (20 mmol) of Boc–γ-Abu–OH **4** was dissolved in a mixture of 10 mL dichloromethane (DCM) in an ice-water bath. H–Val–OMe was isolated from 6.7 g (40 mmol) of the corresponding methyl ester hydrochloride by neutralization, subsequent extraction with ethyl acetate and concentration to 10 mL was done. This extract was added to the reaction mixture, followed immediately by 4.12 g (20 mmol) of dicyclohexylcarbodiimide (DCC). The reaction mixture was allowed to come to room temperature and stirred for 24 h. DCM was evaporated, residue was taken in ethyl acetate (60 mL), and dicyclohexylurea (DCU) was filtered off. The organic layer was washed with 2 M HCl (3 × 50 mL), brine (2 × 50 mL), then 1 M sodium carbonate (3 × 50 mL) and brine (2 × 50 mL) respectively. Then dried over anhydrous sodium sulfate, and evaporated in *vacuo* to yield **5** as a white solid.

Yield = 5.68 g (18 mmol, 90%). (Found: C, 55.7; H, 8.5; N, 8.2%. $C_{15}H_{28}N_2O_5$ (316) requires C, 56.96; H, 8.86; N, 8.86%); ^{1}H NMR (300 MHz, $CDCl_3$) δ 6.61 (Val(2) NH, 1H, d, $J = 6$ Hz); 4.76 (γ-Abu(1) NH, 1H, t); 4.55–4.51 ($C^{\alpha}H$ of Val(2), 1H, m); 3.75 ($-OCH_3$, 3H, s); 3.30–3.14 ($C^{\gamma}Hs$ of γ-Abu(1), 2H, m); 2.46 ($C^{\alpha}Hs$ of γ-Abu(1), 2H, m); 1.95–1.77 ($C^{\beta}Hs$ of γ-Abu(1), 2H, m); 1.67 ($C^{\beta}H$ of Val(2), 1H, m); 1.44 (Boc–CH_3s, 9H, s); 0.97 ($C^{\gamma}Hs$ of Val(2), 6H, m).

(c) Boc–γ-Abu(1)–Val(2)–OH **6**: To 5.05 g (16 mmol) of Boc–γ-Abu(1)–Val(2)–OMe, **5** 20 mL MeOH and 15 mL of 2 M NaOH were added. The reaction mixture was stirred and the progress of saponification was monitored by thin layer chromatography (TLC). After 10 h methanol was removed under *vacuo*, the residue was taken in 50 mL of water, washed with diethyl ether (2 × 50 mL). Then the pH of the aqueous layer was adjusted to 2 using 1 M HCl and it was extracted with ethyl acetate (3 × 50 mL). The extracts were pooled, dried over anhydrous sodium sulfate, and evaporated in *vacuo* to yield **6** as a white solid.

Yield = 4.2 g (14 mmol, 87%). (Found: C, 55.2; H, 8.4; N, 9.15%. $C_{14}H_{26}N_2O_5$ (302) requires C, 55.62; H, 8.6; N, 9.27%); ^{1}H NMR (300 MHz, $(CD_3)_2SO$) δ 12.34 (−COOH, 1H, b); 7.95–7.93 (Val(2) NH, 1H, d, $J = 6$ Hz); 6.81–6.80 (γ-Abu(1) NH, 1H, t); 4.15–4.10 ($C^{\alpha}H$ of Val(2), 1H, m); 2.98–2.86 ($C^{\gamma}Hs$ of γ-Abu(1), 2H, m); 2.50–2.49 ($C^{\alpha}Hs$ of γ-Abu(1), 2H, m); 2.21–2.08 ($C^{\beta}H$ of Val(2), 1H, m); 2.06–1.99 ($C^{\beta}Hs$ of γ-Abu(1), 2H, m); 1.62–1.52 ($C^{\gamma}Hs$ of Val(2), 6H, m); 1.37 (Boc–CH_3s, 9H, s).

(d) Boc–γ-Abu(1)–Val(2)–Leu(3)–OMe **1**: 1.5 g (5 mmol) of Boc–γ-Abu(1)–Val(2)–OH **6** in 10 mL of DMF was cooled in an ice-water bath and H–Leu–OMe was isolated from 1.8 g (10 mmol)

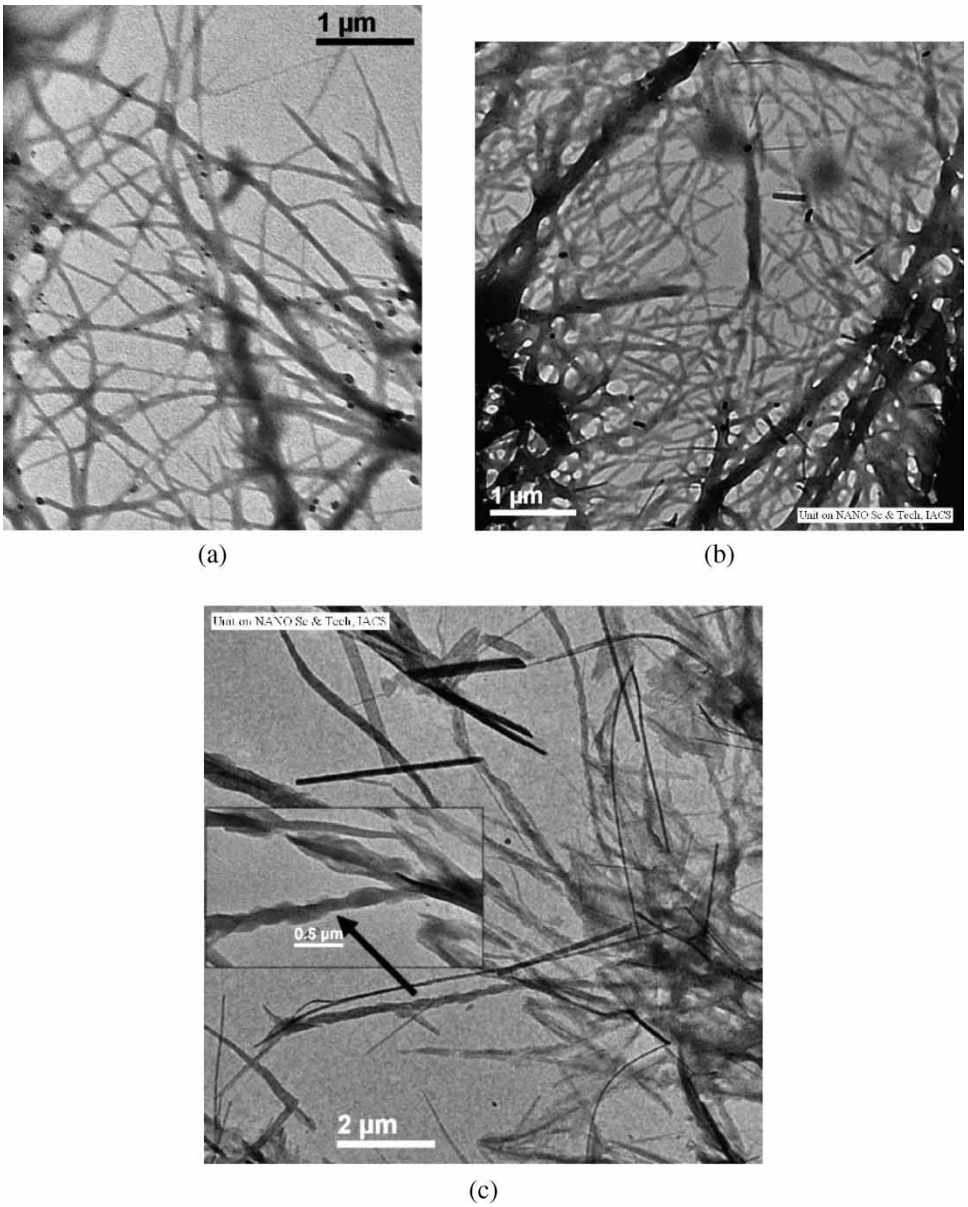

FIGURE 7 Typical TEM images of (a) peptide **1**, (b) peptide **2** and (c) peptide **3** showing nanofibrillar morphology. The inset in Fig. 7(c) indicates the helical nature of the nanofibril. These samples were prepared from slow evaporation of methanol–water solution of peptides on carbon coated copper grid.

of the corresponding methyl ester hydrochloride by neutralization, subsequent extraction with ethyl acetate and concentration to 10 mL was done. The extract was added to the reaction mixture, followed immediately by 1.03 g (5 mmol) DCC and 0.68 g (5 mmol) of HOBt. The reaction mixture was stirred for three days. The residue was taken in ethyl acetate (60 mL) and the DCU was filtered off.The organic layer was washed with 2 M HCl (3 × 50 mL), brine (2 × 50 mL), 1M sodium carbonate (3 × 50 mL) and brine (2 × 50 mL) respectively. Then dried over anhydrous sodium sulfate and evaporated in *vacuo* to yield peptide **1** as a white solid. Purification was done by silica gel column (100–200 mesh) using 3:1 ethyl acetate–toluene as eluent.

Yield = 1.8 g (4.2 mmol, 84%). (Found: C, 58.5; H, 9.0; N, 9.6%. $C_{21}H_{39}N_3O_6$ (429) requires C, 58.74; H, 9.09; N, 9.79%); ^{1}H NMR (300 MHz, $CDCl_3$) δ 6.61 (Leu(3) NH, 1H, d, $J = 9$ Hz); 6.54–6.52 (Val(2) NH, 1H, d, $J = 6$ Hz); 4.78 (γ-Abu(1) NH, 1H, t); 4.65–4.58 (C^{α}H of Leu(3), 1H, m); 4.32–4.27 (C^{α}H of Val(2), 1H, m); 3.72 (–OCH_3, 3H, s); 3.29–3.09 (C^{γ}Hs of γ-Abu(1), 2H, m); 2.30–2.25 (C^{α}Hs of γ-Abu(1), 2H, m); 2.18–2.17 (C^{β}H of Val(2), 1H, m); 1.85–1.76 (C^{β}Hs of γ-Abu(1), 2H, m); 1.68–1.52 (C^{β}Hs & C^{γ}H of Leu(3), 3H, m); 1.44 (Boc–CH_3s, 9H, s); 0.98–0.96 (C^{δ}Hs

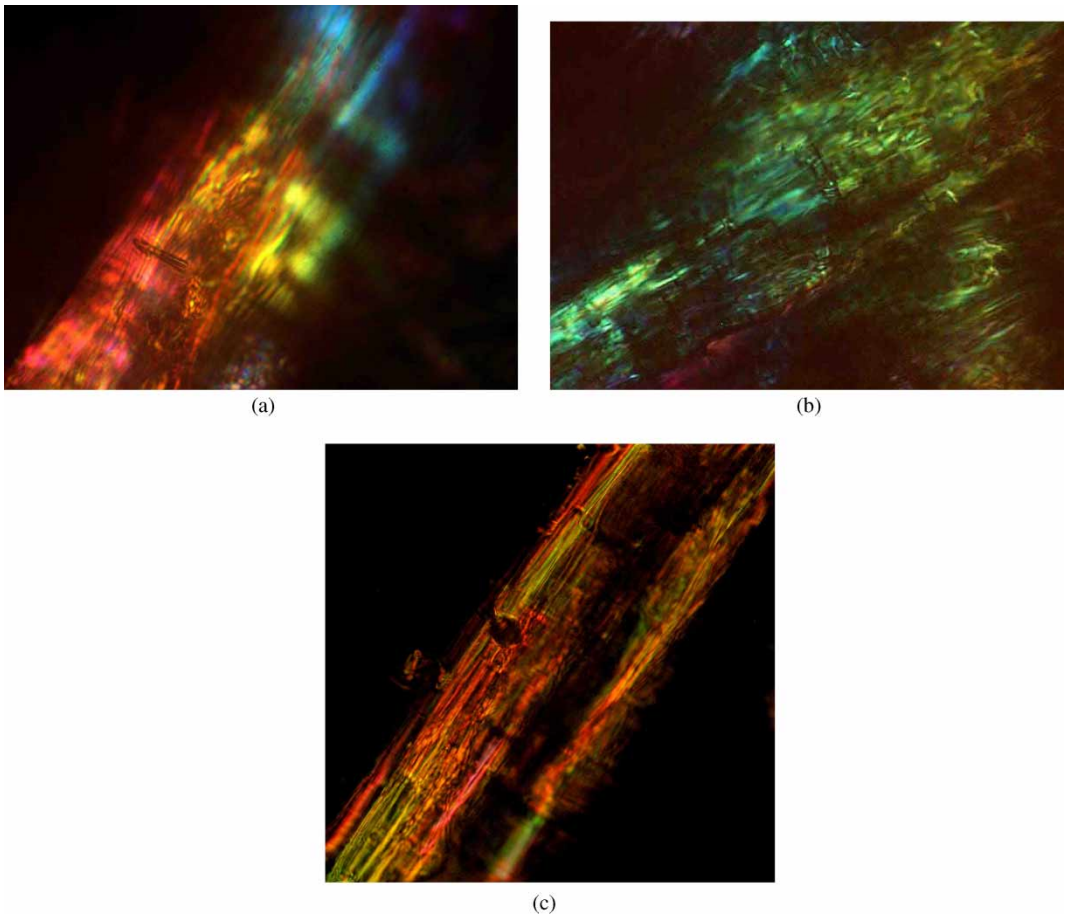

FIGURE 8 Congo red-stained fibrils observed through crossed polarizer showing birefringence, a characteristic feature of amyloid fibrils, for (a) peptide **1**, (b) peptide **2** and (c) peptide **3**.

of Leu(3), 6H, m); 0.94–0.91 (Val(2) C^{γ}Hs, 6H, m); MS (ESI) *m/z* 453 $(M + Na + H)^+$; $[\alpha]_D^{20} = -41.6$ (*c* 0.65, CH_3OH).

(e) Boc–γ-Abu(1)–Leu(2)–OMe **7**: 2.03 g (10 mmol) of Boc–γ-Abu–OH **4** was dissolved in a mixture of 10 mL dichloromethane (DCM) in an ice-water bath. H–Leu–OMe was isolated from 3.63 g (20 mmol) of the corresponding methyl ester hydrochloride by neutralization and subsequent extraction with ethyl acetate and the ethyl acetate extract was concentrated to10 mL. This extract was added to the reaction mixture, followed immediately by 2.06 g (10 mmol) of dicyclohexylcarbodiimide (DCC). The reaction mixture was allowed to come to room temperature and stirred for 24 h. DCM was evaporated, residue was taken in ethyl acetate (60 mL), and dicyclohexylurea (DCU) was filtered off. The organic layer was washed with 2 M HCl (3 × 50 mL), brine (2 × 50 mL), then 1 M sodium carbonate (3 × 50 mL) and brine (2 × 50 mL) and dried over anhydrous sodium sulfate, and evaporated in *vacuum* to yield **7** as a white solid.

Yield = 2.8 g (8.5 mmol, 85%); (Found: C, 57.9; H, 8.9; N, 8.2%. $C_{16}H_{30}N_2O_5$ (330) requires C, 58.18; H, 9.09; N, 8.48%); ^{1}H NMR (300 MHz, $CDCl_3$) δ 6.73 (Leu(2) NH, 1H, d, $J = 9$ Hz); 4.75 (γ-Abu(1) NH, 1H, t); 4.54 (C^{α}H of Leu(2), 1H, m) 3.75 (–OCH_3, 3H, s); 3.19 (C^{γ}Hs of γ-Abu(1), 2H, m); 2.18–2.23 (C^{α}Hs of γ-Abu(1), 2H, m); 1.77–1.82 (C^{β}Hs of γ-Abu(1), 2H, m); 1.92 (C^{β}Hs of Leu(2), 2H, m); 1.62 (C^{γ}H of Leu(2), 1H, m); 1.44 (Boc–CH_3s, 9H, s); 0.90 (C^{δ}Hs of Leu(2), 6H, m).

(f) Boc–γ-Abu(1)–Leu(2)–OH **8**: To 2.64 g (8 mmol) of Boc–γ-Abu(1)–Leu(2)–OMe **7**, 20 mL MeOH and 10 mL of 2 M NaOH were added. The reaction mixture was stirred and the progress of saponification was monitored by thin layer chromatography (TLC). After 10 h methanol was removed under *vacuo*, the residue was taken in 50 mL of water, washed with diethyl ether (2 × 50 mL). Then the pH of the aqueous layer was adjusted to 2 using 1 M HCl and it was extracted with ethyl acetate (3 × 50 mL). The extracts were pooled, dried over anhydrous sodium sulfate, and evaporated in *vacuo* to yield **8** as a white solid.

Yield = 2.21 g (7 mmol, 87.7%); (Found: C, 56.7; H, 8.4; N, 8.55%. $C_{15}H_{28}N_2O_5$ (316) requires C, 56.96; H, 8.86; N, 8.86%); ^{1}H NMR (300 MHz, $(CD_3)_2SO$) δ 8.01–7.98 (Leu(2) NH, 1H, d, $J = 9$ Hz); 6.76 (γ-Abu(1) NH, 1H, t); 4.21–4.13 (C^{α}H of Leu(1), 1H,

m); 2.90–2.84 (C^{γ}Hs of γ-Abu(1), 2H, m); 2.16–2.04 (C^{α}Hs γ-Abu(1), 2H, m); 1.59–1.52 (C^{β}Hs of γ-Abu(1), 2H, m); 1.35 (Boc–CH_3s, 9H, s); 2.48 (C^{β}Hs of Leu(2), 2H, m); 1.49–1.43 (C^{γ}Hs of Leu(2), 1H, m); 0.87–0.80 (C^{δ}Hs of Leu(2), 6H, m).

(g) Boc–γ-Abu(1)–Leu(2)–Phe(3)–OMe **2**: 1.73 g (5.5 mmol) of Boc–γ-Abu(1)–Leu(2)–OH **8** in 10 mL of DMF was cooled in an ice-water bath and H–Phe–OMe was isolated from 2.37 g (11 mmol) of the corresponding methyl ester hydrochloride by neutralization, subsequent extraction with ethyl acetate and concentration to10 mL was done. The extract was then added to the reaction mixture, followed immediately by 1.13 g (5.5 mmol) DCC and 0.74 g (5.5 mmol) of HOBt. The reaction mixture was stirred for three days. The residue was taken in ethyl acetate (60 mL) and the DCU was filtered off. The organic layer was washed with 2 M HCl (3 × 50 mL), brine (2 × 50 mL), 1 M sodium carbonate (3 × 50 mL) and brine (2 × 50 mL) respectively. Then dried over anhydrous sodium sulfate and evaporated in *vacuo* to yield **2** as a white solid. Purification was done by silica gel column (100–200 mesh) using 3:1 ethyl acetate–toluene as eluent.

Yield = 2.14 g (4.5 mmol, 81.67 %); (Found: C, 62.7; H, 8.0; N, 8.4%. $C_{25}H_{39}N_3O_6$ (477) requires C, 62.89; H, 8.17; N, 8.80%); ^{1}H NMR (300 MHz, $CDCl_3$) δ 7.30–7.19 (Aromatic Hs of Phe(3), 5H, m); 7.14–7.11 (Phe(3) NH, 1H, d, $J = 9$ Hz); 6.73–6.70 (Leu(2) NH, 1H, d, $J = 9$ Hz); 6.52 (γ-Abu(1) NH, 1H, t); 4.8–4.75 (C^{α}H of Phe(3), 1H, m); 4.42–4.35 (C^{α}H of Leu(2), 1H, m); 3.71 (–OCH_3, 3H, s); 3.19–3.12 (C^{γ}Hs of γ-Abu(1), 2H, m); 3.09–3.03 (C^{β}Hs of Phe(3), 2H, m); 2.33–2.28 (C^{α}Hs of γ-Abu(1), 2H, m); 2.03–1.92 (C^{β}Hs of Leu(3), 2H, t); 1.85–1.74 (C^{β}Hs of γ-Abu(1), 2H, m); 1.62–1.59 (C^{γ}H of Leu(2), 1H, m); 1.49 (Boc–CH_3s, 9H, s); 1.37–1.15 (C^{δ}Hs of Leu(3), 6H, m); MS (ESI) *m/z* 478 $(M + H)^+$; $[\alpha]_D^{20} = -23.3$ (*c* 0.79, CH_3OH).

(h) Boc–γ-Abu(1)–Val(2)–Tyr (3)–OMe **3**: 1.51 g (5 mmol) of Boc–γ-Abu(1)–Val(2)–OH **6** in 10 mL of DMF was cooled in an ice-water bath and H–Tyr–OMe was isolated from 2.31 g (10 mmol) of the corresponding methyl ester hydrochloride by neutralization, subsequent extraction with ethyl acetate and concentration to 10 mL and it was added to the reaction mixture, followed immediately by 1.03 g (5 mmol) DCC and 0.68 g (5 mmol) of HOBt. The reaction mixture was stirred for three days. The residue was taken in ethyl acetate (60 mL) and the DCU was filtered off. The organic layer was washed with 2 M HCl (3 × 50 mL), brine (2 × 50 mL), 1 M sodium carbonate (3 × 50 mL) and brine (2 × 50 mL) respectively and then dried over anhydrous sodium sulfate and evaporated in *vacuo* to yield **3** as a white solid. Purification was done by silica gel column (100–200 mesh) using 3:1 ethyl acetate–toluene as eluent.

Yield = 1.96 g (4.1 mmol, 82%). (Found: C, 59.9; H, 7.4; N, 8.6%. $C_{24}H_{37}N_3O_7$ (479) requires C, 60.12; H, 7.72; N, 8.76%); ^{1}H NMR (300 MHz, $CDCl_3$) δ 6.99–6.61 (Aromatic Hs of Tyr(3), 4H, m); 6.45–6.42 (Tyr(3) NH, 1H, d, $J = 9$ Hz); 6.15–6.13 (Val(2) NH, 1H, d, $J = 6$ Hz); 4.8 (γ-Abu(1) NH, 1H, t); 4.88–4.82 (C^{α}H of Tyr(3), 1H, m); 4.22–4.13 (C^{α}H of Val(2), 1H, m); 3.75 (–OCH_3, 3H, s); 3.20–3.07 (C^{γ}Hs of γ-Abu(1) & C^{β}Hs of Tyr(3), 4H, m); 2.22–2.18 (C^{α}Hs of γ-Abu(1), 2H, m); 1.95–1.91 (C^{β}Hs of γ-Abu(1), 2H, m); 1.79–1.69 (C^{β}H of Val(2), 1H, m); 1.45 (Boc–CH_3s, 9H, s); 0.93–0.83 (C^{γ}Hs of Val(2), 6H, d); MS (ESI) *m/z* 480 $(M + H)^+$; $[\alpha]_D^{20} = -16.4$ (*c* 0.65, CH_3OH).

NMR Spectroscopy

All NMR studies were carried out on a Brüker DPX 300 MHz spectrometer at 300 K. Peptide concentrations were in the range 1–10 mM in $CDCl_3$ and $(CD_3)_250$.

FT-IR Spectroscopy

The FT-IR spectra were taken using Shimadzu (Japan) model FT-IR spectrophotometer. In the solid state FT-IR studies, powdered peptides were mixed with KBr for preparing thin films.

Mass Spectrometry

Mass spectra were recorded on a Hewlett Packard Series 1100MSD mass spectrometer by positive mode electrospray ionization.

Transmission Electron Microscopic Study

The morphologies of the reported compounds were investigated using transmission electron microscope (TEM). The transmission electron microscopic studies of all the peptides were done using a small amount of the solution (2 mg of peptide in 1 mL of methanol–water (9:1) solution) of the corresponding compounds on carbon-coated copper grids (200 mesh) by slow evaporation and allowed to dry in vacuum at 30 °C for two days. Images were taken at an accelerating voltage of 200 kV. TEM was done by a JEM-2010 electron microscope.

Congo Red Binding Study

An alkaline saturated Congo red solution was prepared. The peptide fibrils were stained by alkaline Congo red solution (80% methanol/20% glass distilled water containing 10 μL of 1% NaOH) for 2 minutes and then the excess stain (Congo red) was removed by rinsing the stained fibril with 80% methanol/20% glass distilled water solution for several times. The stained fibrils were dried in

vacuum at room temperature for 24 hours, then visualized at 40 × or 100 × magnification and birefringence was observed between crossed polarizers.

Single Crystal X-ray Diffraction Study

For peptides **1**, **2** and **3** colorless needle shaped single crystals were obtained from methanol–water solution by slow evaporation. Intensity data for all the peptides were collected with MoKα radiation using the MARresearch Image Plate system. The crystals were positioned at 70 mm from the Image Plate. 100 frames were measured at 2° intervals with a counting time of 2 mins. Data analyses were carried out with the XDS program [37]. The structures were solved using direct methods with the Shelx86 program [38]. Non-hydrogen atoms were refined with anisotropic thermal parameters. The hydrogen atoms bonded to carbon were included in geometric positions and given thermal parameters equivalent to 1.2 times those of the atom to which they were attached. The structures were refined on F^2 using Shelxl [39]. Crystallographic data have been deposited at the Cambridge Crystallographic Data Centre reference CCDC 608786 for peptide **1**, CCDC 608787 for peptide **2** and CCDC 608788 for peptide **3**.

Acknowledgements

This research is supported by a grant from Department of Science and Technology (DST), India (Project No. SR/S5/OC-29/2003). We thank EPSRC and the University of Reading, UK for funds for the Image Plate System. S. Ray and A. K. Das wish to acknowledge the CSIR, New Delhi, India for financial assistance. We gratefully acknowledge the Nanoscience and technology initiative of Department of Science and Technology of Govt. of India, New Delhi for using TEM facility.

References

[1] Banerjee, A.; Maji, S. K.; Drew, M. G. B.; Haldar, D.; Banerjee, A. *Tetrahedron Lett.* **2003**, *44*, 699.
[2] Maji, S. K.; Banerjee, A.; Drew, M. G. B.; Haldar, D.; Banerjee, A. *Tetrahedron Lett.* **2002**, *43*, 6759.
[3] Haldar, D.; Maji, S. K.; Drew, M. G. B.; Banerjee, A.; Banerjee, A. *Tetrahedron Lett.* **2002**, *41*, 5465.
[4] Banerjee, A.; Das, A. K.; Drew, M. G. B.; Banerjee, A. *Tetrahedron Lett.* **2005**, *61*, 5906.
[5] Banerjee, A.; Maji, S. K.; Drew, M. G. B.; Haldar, D.; Das, A. K.; Banerjee, A. *Tetrahedron* **2004**, *60*, 5935.
[6] Das, A. K.; Banerjee, A.; Drew, M. G. B.; Haldar, D.; Banerjee, A. *Supramolecular Chem.* **2004**, *16*, 331.
[7] Maji, S. K.; Drew, M. G. B.; Banerjee, A. *Chem. Commun.* **2001**, 1946.
[8] Hong, Y.; Legge, R. L.; Zhang, S.; Chen, P. *Biomacromolecules* **2003**, *4*, 1433.
[9] Schneider, J. P.; Pochan, D. J.; Ozbas, B.; Rajagopal, K.; Pakstis, L.; Kretsinger, J. *J. Am. Chem. Soc.* **2002**, *124*, 15030.
[10] Pochan, D. J.; Schneider, J. P.; Kretsinger, J.; Ozbas, B.; Rajagopal, K.; Haines, L. *J. Am. Chem. Soc.* **2003**, *125*, 11802.
[11] Lamm, M. S.; Rajagopal, K.; Schneider, J. P.; Pochan, D. J. *Am. Chem. Soc.* **2005**, *127*, 16692.
[12] Yokoi, H.; Kinoshita, T.; Zhang, S. *Proc. Natl. Acad. Sci.* **2005**, *102*, 8414.
[13] Zhang, S. *Nature Biotechnol.* **2003**, *21*, 1433.
[14] Porat, Y.; Stepensky, A.; Ding, F. -A.; Naider, F.; Gazit, E. *Biopolymers* **2003**, *69*, 161.
[15] Porat, Y.; Kolusheva, S.; Jelinek, R.; Gazit, E. *Biochemistry* **2003**, *42*, 10971.
[16] Mazor, Y.; Gilead, S.; Benhar, I.; Gazit, E. *J. Mol. Biol.* **2002**, *322*, 1013.
[17] Reches, M.; Porat, Y.; Gazit, E. *J. Biol. Chem.* **2002**, *277*, 35475.
[18] Lashuel, H. A.; LaBrenz, S. R.; Woo, L.; Serpell, L. C.; Kelly, J. W. *J. Am. Chem. Soc.* **2000**, *122*, 5262.
[19] Deechongkit, S.; Powers, E. T.; You, S. -L.; Kelly, J. W. *J. Am. Chem. Soc.* **2005**, *127*, 8562.
[20] Ryadnov, M. G.; Woolfson, D. N. *Nature Mater.* **2003**, *2*, 329.
[21] Ryadnov, M. G.; Woolfson, D. N. *J. Am. Chem. Soc.* **2005**, *127*, 12407.
[22] Niece, K. L.; Hartgerink, J. D.; Donners, J. J. J. M.; Stupp, S. I. *J. Am. Chem. Soc.* **2003**, *125*, 7146.
[23] Claussen, R. C.; Rabatic, B. M.; Stupp, S. I. *J. Am. Chem. Soc.* **2003**, *125*, 12680.
[24] Sone, E. D.; Stupp, S. I. *J. Am. Chem. Soc.* **2004**, *126*, 12756.
[25] Bull, S. R.; Guler, M. O.; Bras, R. E.; Meade, T. J.; Stupp, S. I. *Nano Lett.* **2005**, *5*, 1.
[26] Gazit, E. *Drugs Fut* **2004**, *29*, 1.
[27] Arriel, R.; Gazit, E. *J. Biol. Chem.* **2001**, *276*, 34156.
[28] Gazit, E. *FASEB J.* **2002**, *16*, 77.
[29] Awapara, J.; Landua, A. J.; Fuerst, R.; Scale, B. *J. Biol. Chem.* **1950**, *187*, 35.
[30] Roberts, E.; Frankels, S. *J. Biol. Chem.* **1950**, *187*, 55.
[31] Maji, S. K.; Banerjee, R.; Velmurugan, D.; Razk, A.; Fun, H. K.; Banerjee, A. *J. Org. Chem.* **2002**, *67*, 633.
[32] Moretto, V.; Crisma, M.; Bonora, G. M.; Toniolo, C.; Balaram, H.; Balaram, P. *Macromolecules* **1989**, *22*, 2939.
[33] Ramachandran, G. N.; Sasisekharan, V. *Adv. Protein Chem.* **1968**, *23*, 284.
[34] Kim, Y. -S.; Randolph, T. W.; Manning, M. C.; Stevens, F. J.; Carpenter, J. F. *J. Biol. Chem.* **2003**, *278*, 10842.
[35] Ryadnov, M. G.; Woolfson, D. N. *Angew. Chem. Int. Ed.* **2003**, *42*, 3021.
[36] Bodanszky, M.; Bodanszky, A. *The Practice of Peptide Synthesis*; Springer-Verlag: New York, 1984; pp 1–282.
[37] Kabsch, W. *J. Appl. Cryst.* **1988**, *21*, 916.
[38] Sheldrick, G. M. *Acta. Crystallogr., Sect. A: Fundam. Crystallogr* **1990**, *46*, 467.
[39] Sheldrick, G. M. *Program for Crystal Structure Refinement*; University of Göttingen: Germany, 1997.